



SEDIMENTOLOGY OF CONVERGENT MARGINS

Taiwan April 26 - May 2

ABSTRACTS

Schedules

Symposium I – April 26th

Venue: Room 213, second floor, Department of Geosciences, National Taiwan University, Taipei

Start	End	Speaker	Title
08:45	09:00	Ludvig Löwemark	Welcome address and introduction to Taiwan
09:00	09:50	Andrew Lin	Keynote: Interplay between tectonics and sedimentation and its resulting stratigraphy of the Taiwan foreland basin: A review
09:50	10:05	Sung-Ping Chang	Millennial- to Centennial-Scale Sequence Stratigraphy in the Choshui River Subaqueous Delta, Offshore Taiwan
10:05	10:20	Tae Soo Chang	Wave-modulated, macrotidal open-estuary tidal bar facies at the Geum River estuary mouth, mid-western coast of Korea: resembling open-coast tidal flats
10:20	10:40	Coffee Break	
10:40	11:30	Annette George	Keynote: Basin Evolution and Paleozoic-Mesozoic terrane assembly in Northern Thailand
11:30	11:45	Zong-Dai Chen	Integrating Microfossil and Geochemical Evidence to Refine the Paleoenvironmental Understanding of the Szekou Formation in southern Taiwan
11:45	12:00	Chelsea Wong	Sedimentary Environment Evolution of the Maobitou Limestone on the Western Hengchun Tableland, Southern Taiwan
12:00	13:00	Lunch	
13:00	13:15	Zhonghao Zhang	The Role of Coccolithophore Deposition in Moving Suspensions: Importance of Flocculation and Its Implication for Modern and Ancient Calcareous Ooze (Chalk) Deposition
13:15	13:30	Juan José Ponce	Recurrence of hyperpycnites in the cenozoic of the foreland Austral Basin, Argentina
13:30	13:45	Milovan Fustic	Potential Genetic Relation of Coal-bearing Foreland and Pull-apart Basins of Central Kazakhstan and Carboniferous Pacific-type Convergent Margin System of the Paleo-Asian Ocean
13:45	14:00	Yechan Park	Three-Dimensional facies architecture and estuary–delta transition in a Holocene tide-influenced system, southern coast of Korea
14:00	14:15	Noelia Carmona (Juan Ponce)	Paleoenvironmental analysis of the Lower Cretaceous Río Mayer Formation (Austral Basin), Argentina

Symposium II – April 29th

Venue: S135 lecture room, Department of Earth Sciences, National Central University, Taoyuan

Start	End	Speaker	Title
08:45	09:00	Andrew Lin	Welcome address
09:00	09:50	Liz Hajek	Keynote: Identifying climate signals in convergent margins: deconvolving signal, noise, and climate-tectonic feedbacks in tectonically active basins
09:50	10:05	Shahin E. Dashtgard	The linked sedimentologic-tectonic evolution of a forearc basin–forearc depression: Georgia Basin, Canada
10:05	10:20	YiSheng Tan	Sapropel, Cyclostratigraphy and Milankovitch cycles: Revisits of Pleistocene GSSPs
10:20	10:40	Coffee Break	
10:40	11:30	Michael Hren	Keynote: Organic molecular paleohypsometry: Promises, pitfalls and implications for the topographic evolution of the Taiwan orogen
11:30	11:45		Open discussion
11:45	12:45	Lunch	

Participant roster

Noelia Carmona, Universidad Nacional de Río Negro

Sung-Ping Chang, National Cheng-Kung University

Tae Soo Chang, Chonnam National University

Zong-Dai Chen, National Taiwan University

Shahin Dashtgard, Simon Fraser University

Milovan Fustic, Nazarbayev University

Annette George, The University of Western Australia

Liz Hajek, Penn State

Michael Hren, University of Connecticut

Yi-Jen Lee, National Taiwan University

Andrew Lin, National Central University

Ludvig Löwemark, National Taiwan University

Yechan Park, Chonnam National University

Juan Ponce, Instituto de Investigación en Paleobiología y Geología (IIPG), CONICET

YiSheng Tan, National Taiwan University

Chelsea Wong, National Taiwan University

Zhonghao Zhang, Indiana University Bloomington

Paleoenvironmental analysis of the Lower Cretaceous Río Mayer Formation (Austral Basin), Argentina

Carmona, N.B.(1,2), Ponce, J.J.(1,2), Cevallos, M.(3), Jait, D.M.(4), Padva, D.(4), Cevallos, M.(3)

1 Instituto de Investigación en Paleobiología y Geología. Consejo Nacional de Investigaciones Científicas y Técnicas. Universidad Nacional de Río Negro. Av. Gral. Julio Argentino Roca 1242, R8332 Gral. Roca, Río Negro, Argentina. ncarmona@urnn.edu.ar

2 Universidad Nacional de Río Negro.

3 Universidad Nacional de San Juan.

4 Compañía General de Combustibles S.A. Gerencia de Exploración, Honduras 5663, CABA, Buenos Aires RC1414BNE, Argentina.

The Río Mayer Formation (Lower Cretaceous) is one of the units that accumulated during the first generalized marine transgression in the back-arc Austral Basin. This formation has been the subject of increasing study in recent years due to its potential as an unconventional reservoir. This study was conducted at Estancia Cristina locality, where this formation comprises a 647 m-thick succession, being the most complete section recorded up to now, for this unit. Four main facies associations have been recognized in this section. FA1 consists mostly of organic-rich mudstones, completely bioturbated, recording the highest TOC values (average 1.5%, maximum 2.17%). These deposits are interpreted as formed in an upper to lower offshore. FA2 is composed of massive marls due to bioturbation with the development of *Zoophycos* ichnofacies, abundant microorganism content, and minimum TOC values (0 to 0.5%). This facies association is interpreted as deposited on an inner shelf. FA3 consists of mudstones and heterolithic mudstones with the development of a *Cruziana* ichnofacies with components of the *Zoophycos* ichnofacies. TOC values range from 0.2% to 1.14%, and it is interpreted as formed in an inner shelf to upper offshore environment. Finally, FA4 comprises marlstones and laminated mudstones, with intercalations of very fine-grained sandstones, without bioturbation and showing the development of extensive levels of microbial mats. This facies association presents TOC values between 0.07% -1.15%, and it is interpreted as deposited in an upper offshore setting. Combined sedimentological, ichnological and geobiological analysis allowed us to infer that oxygen conditions may have fluctuated during the deposition of this unit which affected the establishment of benthos, and that the occurrence of microbial mats was most likely related to upwelling events with expansion of the OMZ, as it occurs in modern analogous.

Millennial- to Centennial-Scale Sequence Stratigraphy in the Choshui River Subaqueous Delta, Offshore Taiwan

Sung-Ping Chang¹, Bo-Hao Shih¹, Jheng-Syun Huang¹, Ho-Han Hsu², Yi-Ping Chen², Arif Mirza²

¹ Department of Earth Sciences, National Cheng-Kung University, Tainan, Taiwan

² Institute of Oceanography, National Taiwan University, Taipei, Taiwan

The Choshui (Zhuoshui) River is an ideal natural laboratory for studying source-to-sink sediment dynamics, owing to its exceptionally high sediment flux relative to its small (~3,000 km²) drainage basin and the presence of active faults. Despite its global significance as an end-member small mountainous river, the Holocene evolution of sediment delivery and its responses to climate variability and tectonic activity remain poorly constrained. The continuous offshore sedimentary archive provides a robust proxy for the upstream fluvial changes. In this study, we utilize high-resolution seismic reflection data (vertical resolution of ~decimeters) to decipher the stratal stacking pattern of the subaqueous delta during the Late Holocene, aiming to gain insights into the environmental parameters within the source-to-sink system.

The high-resolution seismic profiles extending from the river mouth to the offshore area reveal a compound subaqueous delta system, characterized by bathymetric and clinoform features. Based on key bounding surfaces, this subaqueous delta succession is subdivided into five distinct seismic units. Shore-parallel profiles exhibit pronounced onlapping geometries that track the north-south migration of the depocenter, suggesting a Late Holocene river avulsion. The estimated progradation direction is sub-parallel to the onshore transport direction of the Choshui River, indicating a primarily river-dominated setting, though longshore currents gained influence in pro-delta regimes.

Furthermore, analysis of the internal clinoform features resolves two distinct scales of variability. The longer-term cycles manifest as sigmoidal geometries with a concave-up trajectory, reflecting changes in sediment flux. In contrast, a shorter-period cycle is captured by abrupt progradation over every 5-10 m thickness, potentially representing a higher-order depositional sequence. Based on the independent age constraints onshore, preliminary estimates from these stratigraphic hierarchies yield average periodicities on millennial and centennial timescales, respectively. These estimates establish a stratigraphic framework against which future high-resolution dating and paleoclimate records can be tested, offering a rare sedimentary archive linking upstream forcing to offshore depositional response at sub-millennial timescales.

Wave-modulated, macrotidal open-estuary tidal bar facies at the Geum River estuary mouth, mid-western coast of Korea: resembling open-coast tidal flats

Tae Soo Chang, U-Seong Kim, Hun Jun Ha
Department of Geological and Environmental Sciences
Chonnam National University

Estuarine tidal bars are formed by the complex interplay of fluvial, tidal, and wave processes. Open estuary-mouth bars remain understudied compared to their inner-estuary counterparts. This study examines a lobate tidal bar at the Geum River estuary mouth, surrounding Yubu Island, where a central sand spit and coastal dune system bifurcate the bar into a seaward sand flat and a landward mud flat. While the seaward portion operates under a wave-tide mixed-energy regime, the landward section remains tide-dominated. Topographic surveys reveal a convex morphology, with a peak elevation of approximately 3.1 m above MHWL at the central portion, tapering off with gentle gradients. Grain-size analysis shows distinct trends: the sand flat exhibits unimodal frequency with minimal altitudinal variation, whereas the mud flat displays a bimodal, coarsening-upward succession. Seasonal dynamics are pronounced; in summer, mud content increases locally on the sand flat (by 41–90%), while the mud flat surprisingly experiences a 10–25% increase in sand content. Sedimentary facies analysis from box-cores reveals that the sand flat is characterized by hummocky cross-stratification (HCS) and wave ripples with mud drapes, which transition to tide-dominated structures such as current ripples with flaser bedding during summer. The central sand spit exhibits distinct beach facies with alternating heavy- and light-mineral laminations. The landward mud flat is dominated by lenticular bedding, with sand lenses thickening during the summer. The prevalence of wave-induced features and specific grain-size trends suggests that this open-estuary bar closely resembles open-coast tidal flats, with the intervening beach facies serving as a critical diagnostic marker for differentiating these depositional environments.

Integrating Microfossil and Geochemical Evidence to Refine the Paleoenvironmental Understanding of the Szekou Formation in southern Taiwan

Zong-Dai Chen¹, Tzu-Ruei Yang^{2,3,4}, Ludvig Löwemark¹

¹. Department of Geosciences, National Taiwan University, Taipei, Taiwan

². Department of Life Sciences, National Chung Hsing University, Taichung, Taiwan

³. Department of Earth Sciences, National Cheng Kung University, Tainan, Taiwan

⁴. Department of Geology, National Museum of Natural Science, Taichung, Taiwan

The abundant fossil assemblages within the Late Pleistocene Szekou Formation (Hengchun Peninsula, southern Taiwan) suggest a semi-open to open lagoonal system sheltered by barrier islands. However, paleoenvironmental interpretations have long been hindered by dating limitations and uncertainties regarding the spatiotemporal distribution of fossils. While the formation's age is broadly constrained to 30,000-260,000 years, the specific depositional conditions of its fossiliferous intervals remain unclear.

The discovery of a whale skeleton—over 70% complete—offers a unique opportunity to refine the environmental framework of the Szekou Formation. By integrating sedimentological characteristics with molluscan and foraminiferal assemblage analyses, this study reconstructs the paleoenvironmental conditions and constrains the whale-bearing interval to the lowermost part of the Szekou Formation.

Foraminiferal assemblages and planktic/benthic (P/B) ratios indicate fluctuating paleobathymetry between 10–100. The dominance of suspension-feeding bivalves (66%) reflects abundant particulate organic matter (POM) and suggests a productive coastal environment. Together, these results indicate that the paleo-lagoon provided ecological niches favorable for large marine vertebrates. Coarse-grained sediments surrounding the whale fossils, paired with geochemical proxies (C/N ratio: 20.6–23.0; $\delta^{13}\text{C}$: -22.4 to -22.9‰), indicate episodic terrestrial organic matter input. These signatures provide critical insights into the taphonomic conditions contributing to the exceptional preservation.

By combining stratigraphically continuous core materials, stable isotope ratios, and fossil assemblages, this study reconciles previous discrepancies. It clarifies the environmental conditions of the whale's death, the depositional settings favoring its preservation, and the stratigraphic framework of its occurrence.

The linked sedimentologic-tectonic evolution of a forearc basin–forearc depression: Georgia Basin, Canada

Shahin E. Dashtgard, Chuqiao Huang, Maziyar Nazemi, and Francyne Bochi do Amarante

Applied Research in Ichnology and Sedimentology (ARISE) Group, Department of Earth Sciences,
Simon Fraser University, Burnaby, British Columbia, Canada V5A 1S6

The Georgia Basin, Canada and USA has been studied extensively as it records the tectonic evolution of western North America from the Late Cretaceous to today. However, most studies of Georgia Basin strata focused on limited outcrop exposures of Upper Cretaceous strata and this led to the acceptance of a relatively simplistic view of the basin's evolution. Recent studies integrating outcrop and core-based stratigraphic descriptions, 2D seismic, well logs, detrital zircon, and biostratigraphy reveal a complicated depositional history that records both syn-tectonic activity and post-deposition deformation. The fill of the Georgia Basin exceeds 7 km at its deepest point and evidence of syn-sedimentary uplift is recorded in stratigraphic architectures from the Upper Cretaceous through to recent with a general NE-SW trend to structural elements. The strata comprise sediment derived mainly from the adjacent Coast Plutonic Complex.

There was a major shift in depositional environments and drainage patterns from the Late Cretaceous to the Eocene that corresponds to the docking of Siletzia Terrane on North America's western margin. During the Late Cretaceous, sedimentation in the Georgia Basin occurred in deepwater with westward-flowing turbidites. In the Eocene through the Miocene, uplift of the forearc high (Vancouver Island) protected the interior of the Georgia Basin, which was dominated by south through westward flowing rivers in a terrestrial to coastal plain setting. Uplift of the forearc high marked the evolution of the Georgia Basin from a forearc to a forearc depression. The stratigraphic record of the Georgia Basin reveals the close linkage between tectonic activity along North America's active margin and sedimentation responses in the adjacent basin. The Georgia Basin is an example of how a forearc basin can evolve through several different geometries in response to regional tectonic events, and highlights the need to resolve how basin architecture is tied to local tectonic regime.

Potential Genetic Relation of Coal-bearing Foreland and Pull-apart Basins of Central Kazakhstan and Carboniferous Pacific-type Convergent Margin System of the Paleo-Asian Ocean

Milovan Fustic, Yerkebulan Tazabek, Amir Umralin, George Mathews, Mahmoud Leila, Kamal Regmi, and Antoine Dillinger

Nazarbayev University

The geology of Central Kazakhstan comprises a complex assemblage of Proterozoic to Late Paleozoic magmatic, volcanic, and sedimentary successions. The Carboniferous strata hosts Kazakhstan's two largest coal-producing basins, Karaganda and Ekibastuz. The erosional remnants of their age-equivalent ophiolites, basalts, and intrusions, interpreted as Paleozoic intra-oceanic arc formed along a Pacific-type convergent margin are exposed in the Itmurundy, Tekturmas, Zharma, and Char hills. These Late Paleozoic rock-units represent the final accretionary stage of the Neoproterozoic–Late Paleozoic accretionary complex known as Central Asian Orogenic Belt (CAOB), one of the largest and most complex accretionary orogens on Earth.

While the architecture of the paleo-arc orogen is well documented, far less is known about the coeval fold and thrust belt and foreland basin including their sediments. The reasons include: i) poorly preserved rock record as majority of sediments were subsequently reworked; ii) The Karaganda Basin (~3,000 km²) and Ekibastuz Basin (<250 km²) despite decades of large-scale mining exploitations, are lacking modern basin-analysis, provenance, and sedimentological studies.

Examples of our evidences of these basins' potential genetic relation with the Late-Devonian – Carboniferous subduction of the Paleo-Asian Ocean under Kazakhstania plate include:

1. Coeval processes behind two distinct basin types: Karaganda and Ekibastuz basins are characterized by different tectono-stratigraphic framework. The Karaganda (<5km deep wedge-shaped) foreland basin contains dozens of thin (0.5-6m thick) liptinite-free coal seams separated by fluvio-deltaic facies associations; Ekibastuz continental pull-apart basin, contains laterally and vertically dislocated strata within graben-syncline depression and hosts tens of meters thick liptinite-rich coals. The analogy with Pacific-type convergent margin system suggests that these 250km apart from each other coeval basins are most likely simultaneous product of the same oblique arc-continent collision.

2. Syn-depositional volcanic ashfalls: Although volcanic ash is typical of convergent-margin systems, it has not been documented in the Carboniferous basins of Central Kazakhstan. In the Ekibastuz mine, eight suspected tuff layers, each up to 0.5 m thick, are currently being analyzed to determine their provenance and age. These data will help constrain the frequency of explosive volcanism and may guide the search for ash-fall layers in coeval offshore carbonates, where they

could have contributed to supergene copper enrichment.

Strong similarities between CAO B tectonic elements and Karaganda and Ekibastuz basins with the modern convergent-margin accretionary orogen and basins of Taiwan suggests that modern system studies may improve the reconstruction of the Central Kazakhstan's paleo convergent-margins, supporting resource exploration efforts.

Basin Evolution and Paleozoic-Mesozoic terrane assembly in Northern Thailand

Annette George

School of Earth and Oceans, The University of Western Australia

Multiple models have been proposed for amalgamation via collision and accretion of the continental terranes that make up Thailand and neighbouring countries, generating significant debate despite much work over many decades. Geological complexity reflects the collisional events of the Permo–Triassic Indosinian Orogeny, overprinted by the subsequent Himalayan Orogeny. Tropical marine conditions along the (now) western margin of Indochina led to extensive development of Pennsylvanian–Mid Permian mixed carbonate–siliciclastic platforms that are exposed in the Loei-Phetchabun Foldbelt in NE Thailand and intersected by petroleum wells in the deformed subsurface basins beneath the Khorat Plateau. Stratigraphic analysis, carbonate sedimentology and biostratigraphy have been useful for reconstructing stratal architecture in the foldbelt, building on well-described shallow inner platform facies and extensive paleontological work. Interpreting platform evolution has been enhanced by recognition of significant framework-builders, representing outer ramp biostromes and low-relief biostromes, and patch reefs/mounds (platform margin to upper slope deposits) as has recognition of widespread mixed carbonate-siliciclastic slope deposits that link the well-known platform facies with coeval deep basinal deposits. Important tectonic events in platform/basin evolution have been highlighted by detrital zircon provenance data from siliciclastic units and crystallization ages of igneous units recording subduction-related magmatism. The Uttaradit-Nan Suture Zone, located between Indochina and the Sukhothai Arc, has long been considered enigmatic in the collisional history and suturing of Indochina and Sibumasu terrane. Within this suture zone, studies focusing on the Nan Basin have been limited. Detrital zircon geochronology highlights provenance variations across the basin and, in combination with igneous crystallisation ages, supports a back-arc basin origin. Maximum depositional ages constrain timing of closure of the Nan Basin to middle Late Triassic and this timing then also records collision and amalgamation of the Sukhothai Arc and Indochina.

Identifying climate signals in convergent margins: deconvolving signal, noise, and climate-tectonic feedbacks in tectonically active basins

Liz Hajek

Penn State University

Convergent margins can preserve critical information about climate-tectonic coupling and mass fluxes from terrestrial to marine systems. However, complex interactions among sediment supply, accommodation creation, and landscape dynamics on convergent margins make these settings inherently challenging for interpreting the sedimentary record of climate change. Here, we use numerical modeling approaches to explore how coupled feedbacks among tectonics, climate, and sediment-transport systems shape the sedimentary record of climate change on active margins. At the largest scales, a simplified mass-balance model that includes climate-sensitive sediment-transport thresholds shows how, under the same tectonic conditions, wet vs. dry settings record cyclic climate changes in different ways. Margins experiencing climate variability that crosses sediment-transport thresholds can preserve climate signals as identifiable facies changes. In contrast, margins that are either wetter or drier, and are therefore farther from sediment-transport thresholds, instead preserve climate signals as subtle shifts in grain size or shoreline position. At a landscape scale, autogenic sediment-transport dynamics can obscure, overprint, or “shred” climate signals recorded by, for example, geochemical proxies. Stochastic landscape models provide guidelines for overcoming this sedimentary signal shredder through increased sampling. We show that complete paleoclimate records may be recoverable – even in noisy depositional systems – by building composite records from multiple individual records (e.g., outcrop sections or cores) that sample a paleo landscape. Together, these results offer tools for assessing the sensitivity of an active margin setting to record climate change and provide guidelines for study design and sampling to maximize the recovery of paleoclimate signals in deposits from convergent margins.

Organic molecular paleohypsometry: Promises, pitfalls and implications for the topographic evolution of the Taiwan orogen

Michael T. Hren

University of Connecticut

Understanding how mountain belts grow through time requires robust constraints on past topography, yet paleoelevation reconstructions remain challenging in humid, high-relief settings. This talk highlights the application of organic molecular paleohypsometry, a biomarker-based approach that uses the hydrogen isotope composition of fluvially-exported plant leaf waxes to reconstruct catchment-scale elevations, and demonstrates its power for constraining the geomorphic and topographic evolution of active orogens. Because leaf waxes record the hydrogen isotope composition of precipitation during biosynthesis and are transported and integrated across drainage basins, their isotopic signatures preserved in sedimentary archives provide a catchment-averaged record of organic source elevation that is applicable across a wide range of climates and depositional environments. The talk will address key controls on molecular isotope production, transport, and integration, including biomass distribution, erosion efficiency, and sediment routing, and outlines a general framework for applying organic molecular paleohypsometry to other mountain systems worldwide. Finally, this talk will integrate recently published and new Pliocene to recent organic molecular records from eastern Taiwan which provide key constraints on the topographic evolution of the Central Range of Taiwan. Organic molecular isotope data capture significant increases in the mean catchment elevation of river networks draining both southern and central eastern Taiwan in the last ~1.7 Myr and highlight the acceleration of topographic growth along the length of the orogen through the Pleistocene.

Three-Dimensional facies architecture and estuary–delta transition in a Holocene tide-influenced system, southern coast of Korea

Yechan Park

Department of Geological and Environmental Sciences, Chonnam National University

While tectonic uplift, subsidence, and volcanism are primary controls on sedimentation in convergent-margin forearc, backarc, and foreland basins, the evolution of estuarine and coastal systems in tectonically stable settings is predominantly governed by non-tectonic factors, such as climate-driven relative sea-level (RSL) fluctuations and sediment supply rates. In this study, we present the Holocene sedimentary record of a tide-influenced estuary–delta system developed along the southern coast of Korea, and document the facies architecture and stratigraphic evolution pattern of an epicontinental coastal shelf at the marginal sea. Based on sedimentary facies analysis of 6 borehole cores, along with 63 radiocarbon and 14 OSL ages, we identified 27 sedimentary facies grouped into five depositional units: tidal bar (DU1), mudflat/mixed flat (DU2), central bay (DU3), delta front (DU4), and mouth bar (DU5). Stratigraphically, the area exhibits a rapid transition from an estuarine to a deltaic system during the late Holocene. This evolution was primarily driven by RSL fluctuations, variations in sediment supply, and tidal reworking, rather than tectonic subsidence. Specifically, we demonstrate the three-dimensional evolution of the estuary along-strike and down-dip directions, revealing that distinct facies architectures and evolutionary patterns can coexist within a single system where tidal and fluvial processes operate together. These findings suggest a progressive evolution of the estuary–delta transition in tectonically stable settings, contrasting with sedimentary models from active convergent-margin basins where episodic structural forcing dictates sedimentation.

Recurrence of hyperpycnites in the cenozoic of the foreland Austral Basin, Argentina

Juan José Ponce, Noelia Carmona

Instituto de Investigación en Paleobiología y Geología (IIPG), CONICET, Av. J. A. Roca 1242, 8332, General Roca, Argentina.

Universidad Nacional de Río Negro, Instituto de Investigación en Paleobiología y Geología, General Roca, Argentina.

The Cenozoic deep marine deposits of the foreland Austral Basin in Tierra del Fuego, Argentina, show a high frequency of hyperpycnites in their stratigraphic record. The hyperpycnites are density currents produced by river floods, which develop internal arrangements that cannot be modeled by applying the classical turbidite analysis. The sedimentological and ichnological characteristics exhibited by hyperpycnites result from a complex interaction between the morphology of the basin, the duration of the discharges, the fluctuations in flow velocity, and the contribution of fresh water to the basin. These characteristics result in the accumulation of deposits of variable thicknesses, characterized by: 1- a transitional passage, both vertically and laterally, of aggradational and tractive sedimentary structures, which may include granulometric changes and reactivation surfaces, 2- the abundant concentration of particulate organic matter (phytodetritus), and 3- the absence or scarcity of trace fossils, with the development of impoverished ichnofacies. The unusual occurrence of hyperpycnites in the Cenozoic of the foreland Austral basin of Tierra del Fuego is related to its configuration and tectonic evolution. The configuration of the basin, consisting of a supply area (uplifted orogen) close to the accumulation zone and separated by a very narrow transfer area, favored the generation and acceleration of density flows genetically linked to river discharge systems. Tectonic evolution generated two well-defined fill geometries. A ramp system linked to a compressive tectonic regime that ended approximately in the Middle Miocene, which led to the development of a system of prograding clinoforms from the NE. These geometries produced different architectural elements that controlled the distribution of the main sand wedges. The hyperpycnites linked to the ramps are represented by lobe systems fed by small channels of moderate to high sinuosity, while the hyperpycnites associated with the clinoform systems show lobe deposits fed by small channels of high sinuosity in topset positions, and larger channels of low sinuosity at the toe.

Sapropel, Cyclostratigraphy and Milankovitch cycles: Revisits of Pleistocene GSSPs

YiSheng Tan, Ching-En Li, De-Cian Chen, Hao-Ting Yu, Hsing-Yi Yao, & Jih-Pai Lin

National Taiwan University

The Global Boundary Stratotype Section and Point (GSSP), commonly referred to as the “golden spike,” is a geochronological standard established to provide a globally consistent reference framework for stratigraphic correlation. The Mediterranean region preserves a continuous marine stratigraphic record from Pliocene to Holocene, particularly characterized by the alternating occurrence of marls and sapropels. The formation of Mediterranean sapropels is generally attributed to intensified Northern Hemisphere summer insolation driven by precession, which strengthened the African monsoon. The resulting increase in freshwater input reduced or even halted thermohaline ventilation, leading to oxygen depletion in bottom sea water and thereby suppressing organic matter decomposition. The marl-sapropel successions are then can be calibrated and astronomically tuned to Milankovitch cycles. The coding scheme of Mediterranean Precession-Related Sapropels (MPRS), for example, further enhances their potential for global stratigraphic correlation. Among these, the top of sapropel ‘e’ (MPRS 176) in the Vrica Section of Calabria, southern Italy, defines the GSSP for the Calabrian Stage, and it also formerly served as the lower boundary of the Quaternary. The revised base of the Quaternary is now defined at the top of the Nicola Bed (Mediterranean Precession-Related Cycle 250) in the Monte San Nicola section, southern Sicily. During this field trip, four GSSP localities in southern Italy: the Heraclea Minoa section (Zanclean Stage), Punta Piccola section (Piacenzian Stage), Monte San Nicola section (Gelasian Stage), and Vrica section (Calabrian Stage) were visited. Samples were collected from sapropel A5 (the chronological equivalent of the Nicola Bed) and the overlying marl. In addition, samples were collected from sapropel ‘e’ at the Vrica section and the overlying marl.

In term of stratigraphic correlation of Taiwan, the Cholan Formation, owing to the high subsidence and high sedimentation rates of the foreland basin setting in which it accumulated, preserves sea-level changes related to Milankovitch cycles. Recent studies have shown that its stratigraphic cyclicity was influenced by variations in Northern Hemisphere insolation driven jointly by obliquity and precession, suggesting a potential comparability with Mediterranean sapropels, which are likewise linked to precession. By integrating the Mediterranean sapropel framework with existing studies on calcareous nannofossils, magnetostratigraphy, and sequence stratigraphy in the Cholan Formation, it may be possible to identify both the former and current lower boundaries of Quaternary within the Cholan Formation, and to further investigate the influence of Milankovitch forcing and related temporal lags recorded in this succession.

Sedimentary Environment Evolution of the Maobitou Limestone on the Western Hengchun Tableland, Southern Taiwan

Chelsea Wong¹, J. Bruce H. Shyu¹, Shih-Wei Wang², Kai-Shuan Shea³

¹ Department of Geosciences, National Taiwan University, Taipei, Taiwan

² Geology Department, National Museum of Natural Science, Taiwan

³ Geological Survey and Mineral Management Agency, Ministry of Economic Affairs, Taiwan
(retired)

The Hengchun Limestone is an important Quaternary stratigraphic unit in Taiwan, formed offshore the Hengchun Peninsula and uplifted above the sea level during the Penglai orogeny. Although most lithostratigraphic units in the Hengchun Peninsula have been studied, the Maobitou Limestone, a distinctive part of the Hengchun Limestone, has received comparatively little attention. Located at one of the southernmost tips of Taiwan, this unit recorded critical paleoenvironmental information for refining stratigraphic frameworks of the Hengchun Peninsula. The only previous study (Li, 1992) on the Maobitou Limestone proposed its sedimentary environment to be an open shoreface dominated by wave and tidal processes, based on sedimentary structures that were interpreted as large-scale trough, low-angle planar, and herringbone cross-stratifications. However, hummocky cross-stratification (HCS) occurs frequently within this coarse-grained unit, inconsistent with this interpretation. This study examines the Maobitou Limestone through field investigations at 16 coastal outcrops. Three major lithofacies associations were identified: (a) bioclastic packstone facies; (b) bioclastic packstone-grainstone facies; and (c) bioclastic grainstone facies. We interpreted the limestone as a storm-dominated deposit based on six taphonomic indicators: (T1) graded grains within amalgamated beds with HCS; (T2) high abrasion of large bioclastic shell layers; (T3) mixing of planktonic and benthic shell assemblages; (T4) reworked carbonate grain redeposition; (T5) manganese oxide precipitation; and (T6) intensely bioturbated beds beneath HCS. A newly obtained 70-m drill core is also integrated with stratigraphic columns from outcrops, enabling more robust stratigraphic correlation. We also incorporated new

biostratigraphic age determinations to establish a temporal framework for the evolution of sedimentary environments. Through these results, we reconstructed the depositional history of the Maobitou Limestone, and provide a foundation for future correlation between adjacent limestone units across the Hengchun Peninsula. These new data would also have broader implications for Quaternary geological evolution in southern Taiwan.

The Role of Coccolithophore Deposition in Moving Suspensions: Importance of Flocculation and Its Implication for Modern and Ancient Calcareous Ooze (Chalk) Deposition

Zhonghao Zhang

Indiana University Bloomington

Coccolithophores, a group of calcifying phytoplankton, are among the most productive carbonate producers in the oceans. Their remains accumulate to form chalk deposits, which provide unique archives of Earth's geological history. Previous studies have commonly interpreted chalk as a semi-pelagic to pelagic deposit, settling slowly to the seafloor by suspension. Laminated chalk, in particular, has traditionally been explained by meter-scale Milankovitch-paced fluctuations in bottom-water oxygenation, with lamination attributed to intervals of reduced benthic activity under low-oxygen conditions. However, growing sedimentological and ichnological evidence suggests that this interpretation is insufficient. For example, shale was once considered to form exclusively in quiet-water environments, yet physical experiments have demonstrated that fine-grained sediments can aggregate into flocs capable of being transported as bedload. Recent microfacies analyses further indicate that laminated chalk is a product of bottom-current activity. In this study, we use a large racetrack flume facility to conduct physical experiments aimed at understanding the physicochemical properties of coccolithophores and their transport and depositional behavior. Specifically, we investigate the mechanisms of coccolithophore flocculation and quantify the critical velocities required for sediment transport and deposition. Our results demonstrate that bottom-water reworking processes play a key role in the formation of laminated chalk, thereby providing direct insights into pelagic and hemipelagic sedimentary processes.

Itrax Core Scanner description and data sheet

The **Itrax Core Scanner™** determines the variation of all elements from Mg to U along wet as well as dry cores. It offers very high speed of analysis combined with high sensitivity, variable analytical step size and non-destructive scans. The sensor range includes a unique combination of XRF and X-ray radiography, plus high-quality sample images and magnetic susceptibility. Typical applica-

tions include paleoclimate and paleoenvironmental reconstruction, lacustrine and marine sediment studies, quaternary geology, cyclostratigraphy and varve analysis, core correlation and composite sequence construction, drill-core characterization, sedimentology and stratigraphic interpretation

Main benefits

- A unique combination of XRF scanning and X-ray radiography, plus RGB camera and Magnetic Susceptibility in one fully position-calibrated system.
- Very fast XRF scanning at any step size while maintaining high data quality, from centimeter scale and all the way down to sub-millimeter analyses.
- Provides excellent preservation of sensitive samples through non-contact scanning combined with very high analytical speed.
- Measurement of all detectable elements simultaneously in a single scan.
- Excels in proxy studies thanks to very high precision in peak-area determination combined with high sensitivity across a wide range of elements.
- Provides uniquely strong positional precision and repeatability, making it ideal for spliced records and high-resolution stratigraphic studies where position precision is crucial.
- Gives users extended control of the analytical process through easy access to the XRF spectrum from every analytical point.
- Is the leading XRF scanner for sediments examinations worldwide, supported by a large installed base and with extensive scientific publication output of over 200 scientific articles published yearly.
- Is the preferred choice for labs requiring both maximum throughput and the highest performance at millimeter and sub-millimeter resolution.
- Only Itrax Core Scanner maintains the same high data quality per unit time across all resolutions from centimeter scale down to 0.1 millimeter.



Itrax Core Scanner samples are inserted in the left wing, and automatically moved during scanning. The user sets the scan parameters from the computer, and can then leave the instrument to apply the measurements unattended.

Features

The **Itrax Core Scanner™** can scan both wet and dry cores. It offers high sensitivity across a wide elemental range, including the elements commonly used in sediment proxy studies as well as rare earth elements (REEs). The analytical step length can be easily adjusted in the software to meet different resolution requirements, while ensuring continuous coverage over the full step interval and sample length. This makes Itrax equally well suited to rapid sample overviews and high-resolution detailed scans.



This photo shows a split sediment core sample in a liner being placed in the Itrax Core Scanner. The long sample holder allows for all standard core lengths and is easily accessible. All scanning can be performed with or without a foil covering the sample surface, as chosen by the user.

Compatible sample types include wet cores, rock drill cores, slabs, U-channels, peat, cave stones, etc. As long as the samples are reasonably flat, the Itrax follows the surface and automatically adjusts the measurement to a constant distance over the surface.

Only the Itrax scanner family can perform XRF scans that cover all elements, from the lightest to the heaviest, in a single pass.

Itrax does not make direct contact with the sample surface during scanning, but analyzes it from a fixed, close distance.] The advantages include:

- No deformation of soft sediment samples
- The risk of forming a water film between a wet sample and an applied XRF foil is minimized, since no pressing on the film occurs.
- Drying or deformation of the sample between scans is avoided, as can occur in multi-pass scanners that touch the surface.
- Total scan time is minimized by eliminating the need for vertical up-and-down movement at each analytical step.

The combination of XRF and X-ray radiographic imaging enables detailed identification of laminae and clear differentiation between stratigraphic layers and individual particles. This, plus the uniquely precise steps positioning along the sample provides an indispensable examination tool for high-resolution core analysis.

Itrax Core Scanner™ excels in rapid analysis, with performance that has been continuously improved over the years. This high speed is enabled by several features, including the high-power X-ray tube, the very short time between analytical steps, the non-contact measurement principle, and the unique Itrax capability to determine all elements simultaneously at a single voltage. Together, these features reduce scan time to only a fraction of that required by other XRF scanners, without compromising detection limits, quantitative precision, or reproducibility.

Itrax Core Scanner™ provides consistently high analysis speed at every measurement point, regardless of the selected analytical resolution,

from centimeter scale down to sub-millimeter resolution. This unique capability can save substantial scan time, especially when analyzing long samples at millimeter-scale steps or smaller. [The very short time between analytical steps further minimizes total scan time, helping to reduce the time wet samples remain at room temperature.

The digital X-ray radiography system transfers X-ray transmission images directly to the computer. Its advanced design is intended to reveal very small variations in density and chemical composition. X-ray radiography is an ideal complement to the XRF data, helping you verify whether a XRF peak is to be interpreted as, for example, a pebble or as a stratigraphic layer.

The magnetic susceptibility add-on sensor requires contact with the sample surface and is therefore used as the final step in the measurement sequence, when included.

Itrax Core scanner offers uniquely high precision and repeatability in sample positioning, ensuring reliable data at every point, which is crucial, for example, for spliced cores.

The high-quality RGB camera in today's Itrax scanners is equipped with crossed polarizing filters that reduce glare from wet surfaces as well as other surface features that scatter light. The result is high-quality images that reveal details more clearly than the naked eye. The high image quality also enables effective contrast enhancement.

All sensors are position-calibrated relative to one another and operate during scanning with high precision.

Continued on next page

Software ecosystem

The **software package** is developed by Cox and supports the full analytical workflow from acquisition to data review and interpretation.

Itrax Navigator, our software for instrument operation and data display during scanning.

Q-spec, an advanced software package for display of spectra and automated extraction of peak areas for each element, from the x-ray spectra. It separates peaks from background noise and gives you net element peak areas. It also identifies and separates overlapping peaks and identifies sum peaks and diffraction peaks if such appears. It can calculate element concentrations by a simple click, is based on the Fundamental Parameter method and delivers good data from a uniquely wide range of sample matrices with one calibration. Calibrations with other standard samples will only be needed for odd matrix compositions. Another unique Q-spec feature is determination of the average atomic number in the sample

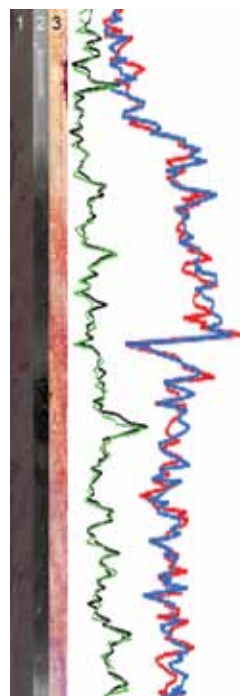
volume, including the elements that are too light to detect with the XRF. This adds further precision to the calculations of element concentrations. The Qspec generates a summary file containing all data from each measurement step together with a note that indicates whether each analysis is correct. This puts the user in control of the analysis at every step. Incorrect data can e.g. be due to the appearance of an unexpected element appearing. XRF spectra from each analytical point is automatically stored for easy user access, review and re-processing.

The **ReDiCore** software is for display and presentation of element profiles, radiographic images, magnetic susceptibility data, and sample photos together.

The **BoreHole Viewer** offers data display and interactive examination of whole boreholes, compiling data from several core scans.

The **data** can be moved seamlessly between the different software apps as well as into e.g. Excel.

This photo shows a 0.1 m. section of a sediment core. Part 1. is the core section as seen by eye. Part 3. been contrast-enhanced. Part 2. in the center is the radiographic image. To the right are four graphs from the XRF scan, showing the variation in concentration along this sample section. The red and the blue graphs show Silica distribution from two consecutive scans. The green and the black graphs show the two Manganese profiles from the two scans. **Please note the very good repeatability in peak position as well as peak size** (arbitrary scale). Measuring time was only 1 second at each position, with 0.2 mm steps. Extending the time improves the precision further. The average Si concentration was ~10%, and Manganese ~0.07%. This core was sampled off Greenland in 2012. Data with courtesy of Dr. R. Gyllencreutz, Stockholm Univ.



Detection limits

Itrax Core Scanner detects all elements across the whole range Mg-U. High sensitivity, well-defined peaks, and high reproducibility for most metals provide the precision needed for confident use of element ratios in proxy studies.

The table lists the Detection Limits for selected elements of common interest. These values are examples spanning light to heavy elements within the full range detectable by

this scanner.] The first value for each element shows the detection limit using a Cr anode

Element PPM	Element PPM	Element PPM
Mg 2230/-	V 16/12	Ba 9/51
Al 4089/575	Mn 24/9	Cd 3/144
Si 2171/1249	Fe 24/9	La 15/47
P 104/465	Br 11/8	Hf 21/51
S 56/204	Rb 12/9	Hg 28/15
K 10/36	Sr 13/9	Pb 25/14
Ca 7/25	Zr 15/73	Th 28/16
Ti 2/14	Mo 14/184	U 35/19

x-ray tube, which has higher sensitivity for

light elements. The second value is the value when applying a Mo tube, offering somewhat better sensitivity for the heavier elements. As a third alternative, a Rh anode x-ray tube can be applied when Mo is of special interest together with other heavier elements (not listed, but available on request). The reference material used is NIST610, measured at 100 seconds, applying the standard scientific model for calculations. Please contact us if you would like information about some element not listed.

Specifications

Function/Parameter	Value/Description
XRF scans and data	Maximum count rate of the XRF detector, up to >300.000 cps, allowing for very fast analyses. Better than 133 eV FWHM at 5.9 keV, at any count rate peak width, for best element peak separation. Typical time setting is 3 (1-10) sec. per scan step for a marine sediment total time per analytical step, covering all detected elements. The time between each measurement step is only a fraction of the time needed in scanners that use up/down movement between each step. The XRF spot size is 0.2 mmx8mm (8mm XRF scan width) as standard, with sharp edges, (0.1mmx8mm beam size optionally).
X-ray radiography	Digital radiography with data fed straight into the computer, resolving variations in sample chemistry and density down to ~0.5%. Image width is ~20 millimeters. Maximum sample thickness depends on composition (~60 mm for a typical marine sediment).
Magnetic Susceptibility	Bartington MS2E type, having a measuring spot of ~4x10mm. Touches sample surface (add-on).
Optical images	High quality RGB images, ~50 micrometer pixel size, an image width of about 100 millimeters, and user selected length along the core. Glare in wet sample photos is minimized by the included crossed polarizing filters.
X-ray Beam	Well defined x-ray beam with 0.2mmx20mm (optionally 0.1mmx20mm) with sharp edges and even intensity distribution. This makes small step analyses down to 0.2/0.1 mm just as fast as larger steps. Larger steps are implemented by sweeping over the selected step, without information loss. Enhanced intensity by Polyflat™ x-ray waveguide speeding up analyses for higher sample throughput.
Scanning steps	Any step from full sample length down to 0.01 millimeter, offering the best available precision in scan step positioning. Allows for continuous scanning without loss of any information along a sample, as well as fast overview by "jumping" between positions at selectable jump length.
Element range and X-Ray tubes	Most users use only one tube type, but Cr, Mo and Rh anode tubes are available as alternatives, depending on elements of most interest for the user. The range is Mg – U for a Cr tube, and Al-U for Mo and Rh tubes. Each tube covers the whole respective element range, with detection limits as described under Detection limits section above. The tubes are easily shifted in ~15 minutes. These high power x-ray tubes are operated at 1650 W for high performance analyses. You are welcome to contact us in case you want more details.
Sample dimensions	Up to 1800 (L) x 122 mm Ø split core / 66 mm full core.
Instrument size and weight	4500 x 820 x 1570 mm LxWxH, ~1100 Kg.
Quantitative calibration	The State-of-the-art element quantification software is pre-calibrated and covers a very wide range of sample matrices. More standards can be added but are only needed for odd sample compositions.
Safety Registration	Ch-08425/S, in Swedish Radiation Safety Authority, plus approved for use in many other countries. The radiation level is below 0.5 µSv/h, allowing for work close to the instrument without limitations.

All specifications and all information in this document are subject to improvements, changes and updates. Please contact us if you want more information.

Itrax FleXRay XRF Scanner description and data sheet

The **ItraxFleXRay XRF Scanner™** determines elemental variations from Na to U along both wet and dry cores. It combines very high analytical speed with high sensitivity across the full elemental range, variable step size, and non-destructive scanning. Typical applications include paleoclimate and paleoenvironmental reconstruction, lacustrine and marine sediment studies, quaternary

geology, cyclostratigraphy and varve analysis, core correlation and composite sequence construction, drill-core characterization, sedimentology and stratigraphic interpretation. The sensor range includes high-quality sample images, magnetic susceptibility and spectrometer options.

Main benefits

- Itrax FleXRay™ combines high-performance XRF scanning with high-quality RGB imaging and, as optional add-ons, magnetic susceptibility and spectrometers in different spectral ranges, with all sensors calibrated to matching lateral positions.
- Itrax scanners offer exceptionally high scanning speed while maintaining high data quality.
- Itrax scanners preserve samples through non-contact scanning and maintain high analytical throughput and data quality in a unique way, even at step sizes down to 1 mm.
- Particularly well suited to proxy studies thanks to high precision in peak-area determination, good sensitivity across a wide range of elements, and precise lateral positioning of the data.
- This XRF scanner delivers high analytical speed without physical contact with the sample. It is especially strong in combining speed and analytical quality at any resolution down to millimeter-scale, and can also be configured for sub-millimeter analytical step sizes.
- Gives the user strong control of the analytical process through easy access to the XRF spectrum from each analytical point.
- Provides high precision in sample positioning at each analytical point, helping ensure that every data value is associated with the correct location.
- Itrax FleXRay Scanner™ is part of the Itrax family of XRF scanners for sediments and drill cores, with installations worldwide and data represented in well over 2,000 scientific publications and a yearly growth in number of articles with more than 200.
- Itrax FleXRay Scanner is well suited to proxy studies because it analyzes a wide range of elements from Na to U with high precision, sensitivity, and variable lateral resolution. Furthermore, all elements are determined in the same XRF scan, under the same analytical conditions, eliminating time-consuming rescans at other voltages and reducing the need for frequent recalibration to normalize data between analytical points.



Itrax FleXRay Scanner offers superb performance, and excels in fast scanning, good sensitivity for a very wide range of elements, combined with cutting edge quantitative capacity.

Features

The **FleXRay Scanner** is a highly useful instrument for preliminary analysis of both wet and dry cores. It offers high sensitivity across a wide element range, with user-selectable step sizes to accommodate different resolution requirements.

Different sample types can be scanned, including wet cores, rock drill cores, slabs, U-channels, peat, cave stones, and related sample types. As long as the samples are reasonably flat, FleXRay follows the sample surface to provide accurate and reproducible analytical data.

Itrax FleXRay is available in two versions: one for both wet and dry samples, and one optimized for dry samples such as drill cores.



The pull-out sample holder makes it convenient, quick and safe to switch samples, whether these are sediments in liners or drill cores.

High sample throughput is a key feature, enabled by fast XRF measurements and very short overhead time between analytical points.

This high scan speed is especially advantageous for high-resolution scanning while still maintaining excellent detection limits, precision, and reproducibility at a typical analysis time of 3 seconds per analytical step. Several features contribute to this performance, including the Cox proprietary X-ray beam guide that increases X-ray intensity at the sample, the short time between analytical steps, the non-contact measurement principle, and the ability to determine all elements at one voltage at each step while maintaining high sensitivity across the full range.

By scanning very close to the sample surface without touching it, the sample is preserved. Together with the high precision of peak-area separation and determination for each element, this is important for the detailed identification of laminae.

Smaller beam size and analytical steps all the way down to 0.2 mm are achieved with the high resolution kit available as an add-on.

Only Itrax scanners perform XRF scans of sediments that cover all elements from Na to U in a single pass. This ensures that all elements are measured under the same analytical conditions. This provides strong detection limits across the full elemental range and avoids time-consuming rescans at other voltages.

Other unique features of Itrax scanners are that

the stability of hardware as well as data processing software make it unnecessary to do frequent re-calibrations during the scans, saving a lot of overhead time during scanning.

Your samples remain minimally affected during and after scanning because Itrax does not come into physical contact with the sample surface. This brings three main advantages: First, pressure on the sample surface is avoided, reducing the risk of deformation in soft samples. Secondly, the risk of forcing water out to form a film between a wet sample and an applied foil is reduced, lowering the risk of adversely affecting the data. Third, the non-contact technique minimizes the time between analytical points, substantially reducing total scan time.

If a magnetic susceptibility sensor is added to your Itrax FleXRay, those measurements are performed last in the analytical sequence, since they require contact with the sample surface and should therefore follow the non-contact measurements.

The RGB camera provides very high-quality images and is equipped with crossed polarizing filters that strongly reduce glare from wet sample surfaces.

Itrax FleXRay scanners offer high precision and repeatability in positioning at each analytical point along the sample. This is needed to ensure correct data at every point, which is important when thickness and absolute positions of laminae are in focus, for instance for spliced core records.

Continued on next page

Software ecosystem

The entire software package is developed by Cox, and includes:

Itrax Navigator, our software for instrument control and real-time data display during scanning.

Q-spec, an advanced software package for spectral display and automated extraction of element peak areas from the X-ray spectra. It also identifies and resolves overlapping peaks, and detects sum peaks and diffraction peaks when they occur. It also identifies and resolves overlapping peaks and detects sum peaks and diffraction peaks when they occur. Element concentrations can be calculated with a simple click; the method is based on Fundamental Parameters and provides robust results across a uniquely wide range of sample matrices using a single calibration. Additional calibrations with other standards are typically only needed for

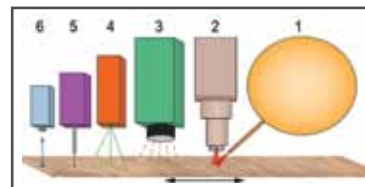
unusual matrix compositions. Another distinctive Q-spec feature is determination of the average atomic number of the analyzed sample volume, including elements too light to be detected directly by XRF. This further improves the precision of the concentration calculations. Q-spec generates a summary file containing all data from each measurement step, together with an indicator showing whether the analysis passed quality checks. This helps keep the user in control of the analytical process at every step. For example, flagged data may result from the presence of an unexpected element. XRF spectra from each analytical point are automatically stored for easy access, review, and reprocessing.

ReDiCore is used to display and present element profiles, radiographic images, magnetic susceptibility data, and sample photographs

together.

BoreHole Viewer enables data display and interactive examination of complete boreholes by compiling data from several core scans

Data can be transferred seamlessly between the different software applications and into programs such as Excel.]



This image shows the principal setup of the Itrax FlexRay x-ray source and sensors.

1. X-ray tube with Polyflat™ x-ray optics. 2. XRF detector. 3. RGB camera. 4. Laser distance gauge. 5. Spectrometer. 6. Magnetic susceptibility sensor.

Detection limits

Itrax FlexRay Scanner detects elements across the full range from Na to U. High sensitivity, well-defined peaks, and high reproducibility for most metals provide the precision needed for confident use of element ratios in proxy studies.

The table lists detection limits for selected elements of common interest. These values are examples spanning light to heavy elements within the full range detectable by this scanner. Na, Mg, and Al are listed with two values because the

FlexRay version for wet sediments has somewhat higher detection limits for these

Element PPM	Element PPM	Element PPM
Na 1251/3720	Ti 8	Ba 23
Mg 191/212	V 7	Cd 64
Al 56/60	Mn 6	La 21
Si 30	Br 5	Hf 10
P 22	Rb 5	Hg 9
S 12	Sr 6	Pb 9
K 11	Zr 6	Th 11
Ca 9	Mo 6	U 12

elements. The second value for Na, Mg and Al refers to the FlexRay version for wet and dry samples.

The reference material used is NIST 610, measured at 100 seconds, applying the standard scientific model for the calculations. *Please contact us if you would like information on any specific element not listed here.*

Specifications

Function/Parameter	Value/Description
XRF scans and data	Typical time setting is 3 (1-10) sec. per scan step for a marine sediment total time per analytical step, covering all detected elements. The XRF spot size is 1mmx8mm (8mm XRF scan width) as standard, (0.2mmx8mm with optional equipment). Maximum count rate of the XRF detector is >300,000 cps, allowing for samples with varying matrices without saturation effects. Better than 134 eV XRF detector FWHM at 5.9 keV, at any count rate peak width. This allows for very good peak separation and minimized overlap. The overhead time between each XRF step is ~0.7 sec.
Magnetic Susceptibility	Bartington MS2E type, having a measuring spot of ~4x10mm. Touches sample surface (add-on).
Optical images	High quality RGB images, ~50 micrometer pixel size, and an image width of ~100 millimeters. Image quality reductions like glare in wet sample photos and light scatter from rough dry surfaces is minimized by the implemented crossed polarizing filters.
X-ray Beam	Well defined x-ray beam with 1mmx8mm, having sharp edges and an even intensity distribution. Enhanced intensity by Polyflat™ x-ray waveguide speeding up analyses for higher sample throughput.
Scanning steps	Any step from full sample length down to 0.01 millimeter can be selected. Step sizes larger than the beam are implemented by sweeping over the selected step, without information loss. This makes any step size analyses down to 1mm just as fast as larger steps, as larger steps than beam size are achieved by collecting data while sweeping over the selected step. Itrax FlexRay allows for scanning without loss of any information along a sample, and also allows for fast overview through discreet analysis mode, by "jumping" between positions at user selectable jump length and analytical step length.
X-Ray tube	A 60W Rh anode tube with an expected life time of 50,000 hours.
Element range	Na – U for wet and dry samples, determined simultaneously.
Sample dimensions	Up to 1520 (L) x 127 mm Ø split and full core.
Instrument size and weight	~2800x1350x1725 millimeters LxWxH including stand, plus top light. The weight is ~700 kilos.
Quantitative calibration	Peak areas and element concentrations are both available for the user, by a single click. The State-of-the-art element quantification software is pre-calibrated and covers a very wide range of sample matrices without further calibrations. More standards can be added, but are only needed for odd sample compositions.
Safety Registration	Ch-08425/S, in Swedish Radiation Safety Authority, plus is approved for use in many other countries. The dose rate equivalent level is below 0.5 µSv/h, allowing for work close to the instrument without limitations.
Power requirement	As standard 230 volts / 50-60Hz / 16 A one phase / 3KW. Other voltages and/or frequencies can be delivered on request
Available add on's	1. High resolution scanning kit that allows the user to switch beamsize to 0.2 mm. beam, for scanning in the 0.2-0.9 mm range. 2. Magnetic Susceptibility meter Bartington MS2E type, having a measuring spot of ~4x10mm. Touches sample surface. 3. Spectrometer with a choice of configurations. Please contact us for more details.

All specifications and all information in this document are subject to improvements, changes and updates. Please contact us if you want more information.

SPONSORS

